5288 *Inorg. Chem.* **2009**, *48*, 5288–5295
DOI: 10.1021/ic900261s

Inorganic Chemistry
Article

Development of Five-Coordinate Zinc Mono- and Dithiolates as S-Donor Metalloligands: Formation of a Zn−W Coordination Polymer

Elky Almaraz,[†] William S. Foley,[†] Jason A. Denny,[†] Joseph H. Reibenspies,[†] Melissa L. Golden,[‡] and Marcetta Y. Darensbourg*,[†]

[†]*Department of Chemistry, Texas A&M University, College Station, Texas 77843, and* [‡]*Department of Chemistry, California State University, Fresno, California 93740*

Received February 6, 2009

The synthesis and isolation of mono- and dithiolate-bridged $\mathrm{Zn}(\mu\text{-SR})_n\mathrm{W(CO)}_m$ (where $n = 1$, $m = 5$; $n = 2$, $m = 4$) species from the dimeric *N,N'*-bis(2-mercaptoethyl)-1,4-diazacycloheptanezinc(II), **[Zn-1′]$_2$**, and the monomeric [*N*-(3-thiabutyl)-*N'*-(3-thiapentaneoate)-1,5-diazacycloheptane]zinc(II), **Zn-1′-Ac**, are described. Upon cleavage of the dimeric **[Zn-1′]$_2$** with $\mathrm{Na^+[ICH_2CO_2]^-}$, the resulting **Zn-1′-Ac** product is isolated as a monomeric, five-coordinate $\mathrm{Zn(N_2SS'O)}$ complex equipped with one available Zn-bound thiolate for further reactivity. Cleavage of **[Zn-1′]$_2$** with $\mathrm{[Et_4N]^+Cl^-}$ afforded a monomeric intermediate, **[Zn-1′-Cl]$^-$**, containing two Zn-bound thiolates. The zinc mono- and dithiolato complexes demonstrated reactivity toward labile-ligand tungsten carbonyl species, $\mathrm{(THF)W(CO)_5}$ and $\mathrm{(pip)_2W(CO)_4}$, to yield respectively **[(Zn-1′-Ac)W(CO)$_5$]$_x$** and **[(Zn-1′-Cl)W(CO)$_4$]$^-$** complexes that were isolated and characterized spectroscopically and via X-ray diffraction. Upon binding to $\mathrm{W(CO)_5}$, the five-coordinate $\mathrm{Zn(N_2SS'O)}$ complex becomes six-coordinate within the coordination polymer **[(Zn-1′-Ac)W(CO)$_5$]$_x$**, in which the acetate tether of each molecule provides an O donor to occupy the octahedral axial position of a neighboring moiety. The **[(Zn-1′-Cl)W(CO)$_4$]$^-$** dithiolate-bridged complex maintains a five-coordinate, square-pyramidal $\mathrm{[Zn(N_2S_2Cl)]^-}$ center, utilizing a chloride as the apical donor and resulting in an overall anionic complex. The addition of CO(g) to the **[(Zn-1′-Cl)W(CO)$_4$]$^-$** complex was monitored by IR spectroscopy, which showed the emergence of **[(Zn-1′-Cl)W(CO)$_5$]$^-$**.

Introduction

Zinc(II), a ubiquitous ion that is essential for all life forms, has established its importance in biology through both structural and catalytic purposes.[1,2] As a borderline hard/soft metal ion with no strong geometrical preferences, N-, S-, and O-donor sets are commonly observed in biological systems.[3,4] Zinc thiolate reactivity, such as cysteine S-alkylation, plays a significant role in the function of proteins such as cobalamin-independent and -dependent methionine synthase, farnesyl transferase, and the Ada repair protein.[5−7] The exploration of zinc thiolates encompasses a wide range of synthetic models that seek to elucidate the reactivity of such spectroscopically silent species. There is an established library of known synthetic models for these sites, especially for the Zn site within the *Escherichia coli* Ada protein, which is responsible for the repair of DNA alkyl phosphotriester lesions through alkyl group transfer to the S of a Zn-bound thiolate. Small-molecule analogues, such as $\mathrm{[Zn(SC_6H_5)_4]^{2-}}$ and zinc tripodal complexes, have been examined for their $\mathrm{SR^-}$ reactivity via alkylation studies.[8−10] Other Zn-containing models have developed tetradentate $\mathrm{N_2S_2}$ ligands that position Zn in a secure square-pyramidal or distorted tetrahedral environment for investigations on the reactivity of their Zn−S sites.[11−13]

The preorganization of multidentate $\mathrm{N_2S_2}$ ligands, as implemented in the present study, maintains the structural integrity of the coordination complex and allows for modification of the terminal thiolate S atoms by metalation or oxygenation while remaining Zn-bound. Certain metalloenzyme active sites containing cysteinyl thiolates are known

---

*To whom correspondence should be addressed. E-mail: marcetta@mail.chem.tamu.edu.

(1) *Nature's Building Blocks: An A−Z Guide to the Elements*; Emsley, J., Ed.; Oxford University Press: Oxford, U.K., 2003; pp 499−505.
(2) Berg, J. M.; Shi, Y. *Science* **1996**, *271*, 1081–1085.
(3) Maret, W. *Antioxid. Redox Signaling* **2006**, *8*, 1419–1441.
(4) Karlin, S.; Zhu, Z.-Y. *Proc. Natl. Acad. Sci. U.S.A.* **1997**, *94* 14231–14236.
(5) Maret, W. *Biochemistry* **2004**, *43*, 3301–3309.
(6) Matthews, R. G.; Goulding, C. W. *Curr. Opin. Chem. Biol.* **1997**, *1*, 332–339.
(7) Hightower, K. E.; Fierke, C. A. *Curr. Opin. Chem. Biol.* **1999**, *3* 176–181.
(8) Parkin, G. *Chem. Rev.* **2004**, *104*, 699–767.
(9) Vahrenkamp, H. *Dalton Trans.* **2007**, 4751–4759.
(10) Wilker, J. J.; Lippard, S. J. *Inorg. Chem.* **1997**, *36*, 969–978.
(11) Grapperhaus, C. A.; Tuntulani, T.; Reibenspies, J. H.; Darensbourg, M. Y. *Inorg. Chem.* **1998**, *37*, 4052–4058.
(12) Grapperhaus, C. A.; Mullins, C. S.; Kozlowski, P. M.; Mashuta, M. S. *Inorg. Chem.* **2004**, *43*, 2859–2866.
(13) Grapperhaus, C. A.; Mullins, C. S.; Mashuta, M. S. *Inorg. Chim. Acta* **2005**, *358*, 623–632.

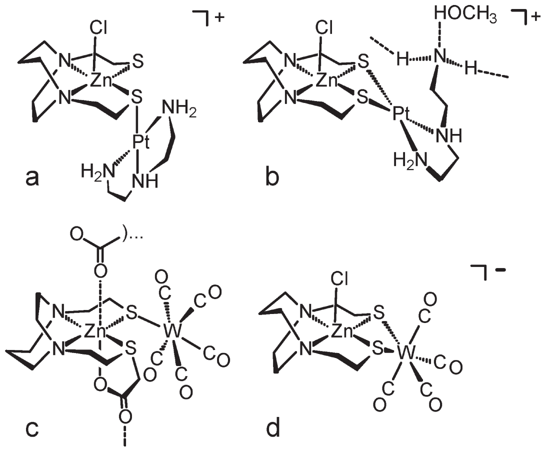

Figure 1. Zn−Pt and Zn−W mono- and dithiolate-bridged complexes: (a) [(Zn(bme-dach)Cl)(Pt(dien))]$^+$ monothiolate-bridged adduct, supported by ^{195}Pt NMR spectroscopy;[18] (b) [(Zn(bme-dach)Cl)(Pt(dien))]$^+$ dithiolate-bridged adduct with a dangling amine stabilized by a network of hydrogen bonding, confirmed by ^{195}Pt NMR spectroscopy and X-ray crystallography;[18] (c) **(Zn-1′-Ac)W(CO)$_5$** monothiolate-bridged unit within a coordination polymer; (d) **[(Zn-1′-Cl)W(CO)$_4$]$^-$** dithiolate-bridged complex.

to be post-translationally modified by oxygenation (nitrile hydratase) or metalation (acetyl coA synthase).[14,15] While post-translational modifications have not yet been discovered for biomolecules containing zinc thiolates, S-metalation has been proposed to be involved in ternary complexes of Zn-finger proteins and Pt-bound DNA.[16] Explorations of the possible molecular interactions have employed **[Zn-1′]$_2$** as a biomimetic for cysteine-rich Zn-finger sites and [Pt(N$_3$Cl)]$^+$ complexes as models of Pt-bound DNA to yield discrete complexes containing Zn−(μ-SR)−Pt bridges, along with Zn/Pt metal-exchanged products.[17,18] These investigations have been based on the notion that modification of the Zn−S sites, whether by alkylation, oxidation, or metalation, may disrupt the overall structure of the zinc proteins, thus altering and/or inhibiting their critical biological functions.[19] Furthermore, such zinc proteins have been explored as drug targets in the treatment of cancer and HIV.[20−23]

Parts a and b of Figure 1 display the mono- and dithiolate-bridged Zn−(μ-SR)−Pt products that resulted from the reaction of **[Zn-1′]$_2$** and [Pt(dien)Cl]Cl at 37 °C. Through ^{195}Pt NMR spectroscopy, parts a and b were observed to exist in equilibrium in the reaction solution (MeOH), yet the dithiolate-bridged species (part b) was the sole product detected in the crystals resulting from the product solution as determined by single crystal X-ray diffraction.

To our knowledge, this Zn−(μ-SR)−Pt-bridged species, [(Zn(bme-dach)Cl)(Pt(dien))]Cl, has been the first structurally isolated Zn−Pt bimetallic thiolate-bridged model that demonstrates the interaction between Zn-bound thiolates and Pt^{2+}.

To provide a broader base of Zn−(μ-SR)−M interaction possibilities and to further the understanding of zinc thiolates as S-donor ligands to heavy metals, the present study (1) implements similar Zn−S complexes and S-modified derivatives, (2) employs an exogenous heavy metal, tungsten, that is not likely to replace zinc within the ligand chelate, and (3) incorporates carbonyl ligands about the tungsten to allow for IR spectral reporting via ν(CO) stretching frequencies. Parts c and d of Figure 1 show the mono- and dithiolate-bridged Zn−W complexes to be discussed within the present paper. To target and isolate a monothiolate-bridged adduct (c), the Zn-(N$_2$SS′O) complex (where S = thiolate and S′ = thioether) was used as the metalloligand for bridging to the tungsten carbonyl moiety via one thiolate. Herein, the synthesis, characterization, and spectral and structural properties of the Zn-(N$_2$SS′O), or **Zn-1′-Ac**, and Zn(μ-SR)$_n$W(CO)$_m$ (where n = 1, m = 5; n = 2, m = 4) adducts will be described in detail.

Experimental Section

Methods and Materials. All solvents used were reagent grade and were dried and distilled under N$_2$ using standard techniques. The *N*,*N*′-bis(2-mercaptoethyl)-1,4-diazacycloheptanezinc(II) dimer[18] and *cis*-(pip)$_2$W(CO)$_4$ (pip = piperidine)[24] were prepared according to published procedures. All reactions were carried out under an inert atmosphere unless otherwise noted.

Physical Measurements. Elemental analyses were performed by Canadian Microanalytical Services, Ltd., Delta, British Columbia, Canada (**[(Zn-1′-Ac)W(CO)$_5$]$_x$**), and Atlantic Microlab, Inc., Norcross, GA. Electrospray ionization mass spectrometry (ESI-MS) spectra were obtained in the Laboratory for Biological Mass Spectrometry at Texas A&M University. IR spectra were recorded on a Bruker Tensor 37 Fourier Transform infrared (FTIR) spectrometer, using a CaF$_2$ cell with a 0.1 mm path length for solution analysis and an attenuated total reflectance attachment equipped with a ZnSe crystal for solid sample analysis. Photolysis experiments were performed using a Newport Oriel Apex Illuminator 100 W Hg UV lamp. Thermogravimetric analysis (TGA) was performed on an Instrument Specialists Inc. TGA 1000 thermogravimetric analyzer and monitored over a range of 22−300 °C at increases of 1 °C/min.

Synthesis of [*N*-(3-Thiabutyl)-*N*′-(3-thiapentanoate)-1,4-diazacycloheptane]zinc(II), Zn(tbtp-dach), Zn-1′-Ac. A portion of **[Zn-1′]$_2$** (0.171 g, 0.301 mmol) was placed in a degassed 500 mL Schlenk flask equipped with a reflux condenser, followed by the addition of 200 mL of CH$_3$OH. As the suspension was stirred at room temperature, a solution of Na$^+$[ICH$_2$CO$_2$]$^-$ (0.134 g, 0.644 mmol) dissolved in 25 mL of CH$_3$OH was added via cannula. The reaction mixture was refluxed in an oil bath held at 80 °C overnight under N$_2$. After cooling to 22 °C, the solution was filtered to remove solids and the filtrate was placed in a rotary evaporator for solvent removal. The resulting white solid was purified by a silica gel chromatography column (5 cm × 20 cm) with CH$_3$OH as the eluent to remove NaI. The hygroscopic, air-stable product was dried to yield 0.172 g (0.503 mmol, 83.6%) and recrystallized by vapor diffusion of diethyl ether into a CH$_3$OH solution. ESI-MS spectrum: m/z = 363 ([M + Na]$^+$). IR (in CH$_3$CN, cm^{-1}): 1636 (s, br), 1445 (vs), 1420 (shoulder), 1375 (vs, sharp). Elem. anal.

---

[14] Darnault, C.; Volbeda, A.; Kim, E. J.; Legrand, P.; Vernede, X.; Lindahl, P. A.; Fontecilla-Camps, J. C. *Nat. Struct. Biol.* **2003**, *10*, 271–279.

[15] Song, L.; Wang, M.; Shi, J.; Xue, Z.; Wang, M.-X.; Qian, S. *Biochem. Biophys. Res. Commun.* **2007**, *362*, 319–324.

[16] Anzellotti, A. I.; Liu, Q.; Bloemink, M. J.; Scarsdale, J. N.; Farrell, N. *Chem. Biol.* **2006**, *13*, 1–10.

[17] Liu, Q.; Golden, M.; Darensbourg, M. Y.; Farrell, N. *Chem. Commun.* **2005**, *34*, 4360–4362.

[18] Almaraz, E.; de Paula, Q. A.; Liu, Q.; Reibenspies, J. H.; Darensbourg, M. Y.; Farrell, N. P. *J. Am. Chem. Soc.* **2008**, *130*, 6272–6280.

[19] Hanas, J. S.; Larabee, J. L.; Hocker, J. R. Zinc Finger Interactions with Metals and Other Small Molecules. In *Zinc Finger Proteins: From Atomic Contact to Cellular Function*; Iuchi, S., Kuldell, N., Eds.; Landes Bioscience: Austin, TX, 2005; pp 39−46.

[20] Beerheide, W.; Bernard, H. U.; Tan, Y. J.; Ganesan, A.; Rice, W. G.; Ting, A. *J. Natl. Cancer Inst.* **1999**, *91*, 1211–1220.

[21] Farrell, N. F. *Coord. Chem. Rev.* **2002**, *232*, 1–4.

[22] Garcia, C. C.; Damonte, E. B. *Infect. Disord. Drug Targets* **2007**, *7*, 204–212.

[23] Lazarczyk, M.; Favre, M. *J. Virol.* **2008**, *82*, 11486–11494.

[24] Darensbourg, D. J.; Kump, R. L. *Inorg. Chem.* **1978**, *17*, 2680–2682.

Table 1. Elemental Analyses of **[(Zn-1′-Ac)W(CO)$_5$]$_x$**

	calculated			found	
	$C_{16}H_{20}N_2S_2O_7W_1Zn_1$	−CO	−2CO	sample 1	sample 2
C	28.87	28.25	27.58	27.88	27.40
H	3.03	3.16	3.31	3.57	3.15
N	4.21	4.39	4.59	4.74	3.95

Calcd (found) for $C_{11}H_{20}N_2S_2O_2Zn_1$ (MW = 341.8 g/mol): C, 38.65 (38.56); H, 5.90 (6.04); N, 8.20 (7.86). Mp: 126−127 °C.

Synthesis of *N*,*N*′-Bis(2-mercaptoethyl)-1,4-diazacycloheptanezinc(II) Acetate−Tungsten Pentacarbonyl Coordination Polymer, [(Zn-1′-Ac)W(CO)$_5$]$_x$. A suspension of W(CO)$_6$ (0.074 g, 0.211 mmol) in 65 mL of tetrahydrofuran (THF) was photolyzed for 2 h under an Ar flow to produce a clear, golden solution of (THF)W(CO)$_5$ [2075 (vw), 1930 (s), 1891 (w) cm^{-1}]. The solution was transferred via cannula to a stirring suspension of **Zn-1′-Ac** (0.072 g, 0.211 mmol) in 5 mL of THF. The mixture was stirred for 3.5 h at 22 °C, and the reaction was monitored via IR spectroscopy. The resulting clear, bright-yellow solution, with ν(CO) IR bands as listed below, was filtered anaerobically. Hexanes were added to the filtrate to precipitate a yellow powder. The flask was placed in the freezer (−20 °C) to assist in further precipitation of the product. The solid was isolated via anaerobic filtration, washed three times with hexane, and dried under an Ar flow to yield 0.040 g (0.060 mmol, 28.4%). The product was redissolved in THF and layered with hexanes to yield yellow X-ray-quality crystals. IR (THF, cm^{-1}): acetate, 1653 (s, br), 1460 (vs, sharp), 1365 (m); ν(CO), 2065(vw), 1925(s), 1888(w). IR [*N*,*N*-dimethylformamide (DMF), cm^{-1}]: ν(CO), 2065(vw), 1921(s), 1871(w). IR (solid state, cm^{-1}): acetate, 1592 (s), 1462 (m, sharp), 1365 (m); ν(CO), 2059(vw), 1910(s), 1867(w), 1807 (shoulder). Mp: 240−280 °C (dec).

Elem. anal. Calcd for $C_{16}H_{20}N_2S_2O_7W_1Zn_1$ (MW = 665.8 g/mol): Samples from two preparations both showed better matches with CO loss, as displayed below in Table 1.

TGA of the **[(Zn-1′-Ac)W(CO)$_5$]$_x$** solid indicated 4.6% weight loss at 42−140 °C (loss of one CO ligand = 4.2% mass). Above 140 °C, the thermal decomposition curve displays a steady decrease in mass with no stability plateaus.

Synthesis of [Tetraethylammonium][*N*,*N*′-Bis(2-mercaptoethyl)-1,4′-diazacycloheptane]zinc(II)−Chlorotungsten Tetracarbonyl, [Et$_4$N][(Zn-1′-Cl)W(CO)$_4$]. In a 100 mL Schlenk flask, a sample of **[Zn-1′]$_2$** (0.154 g, 0.271 mmol) and Et$_4$NCl (0.101 g, 0.610 mmol) was degassed prior to the addition of 25 mL of dry CH$_2$Cl$_2$. The cloudy suspension was stirred for 10 min, at which time it became clear and colorless. A solution of *cis*-(pip)$_2$W(CO)$_4$ (0.265 g, 0.570 mmol) in 35 mL of CH$_2$Cl$_2$ was slowly cannulated into the stirring Zn solution. After 3 h, the solution was anaerobically filtered, and hexanes were added to the filtrate to precipitate a yellow powder. The yellow product was isolated via anaerobic filtration, washed twice with benzene, and dried under a N$_2$ flow to yield 0.298 g (0.400 mmol, 73.8%). The product was dissolved in CH$_2$Cl$_2$ and layered with hexanes to yield yellow X-ray-quality crystals. IR (DMF, cm^{-1}): ν(CO), 1988 (w), 1861 (s), 1836 (m), 1801 (m). IR (CH$_2$Cl$_2$, cm^{-1}): ν(CO), 1990 (w), 1863 (s), 1845 (m), 1800 (m). Elem. anal. Calcd (found) for $C_{21}H_{38}N_3S_2O_4Cl_1W_1Zn_1$ (MW = 745.4 g/mol): C, 33.84 (33.04); H, 5.14 (5.38); N, 5.64 (5.44). Mp: 70−115 °C (dec) color change to brown; 215 °C (dec) color change to black.

X-ray Structure Analysis. The X-ray data for the three structures were obtained in the X-ray Diffraction Laboratory at Texas A&M University. Low-temperature (110 K) X-ray diffraction data were collected on a Bruker SMART 1000 CCD-based diffractometer (Mo Kα radiation, λ = 0.710 73 Å) for **Zn-1′-Ac**.[25] The data for **[Et$_4$N][(Zn-1′-Cl)W(CO)$_4$]** were collected on the Bruker-AXS APEX-II CCD three-circle X-ray diffractometer under the same conditions. For the **[(Zn-1′-Ac)W(CO)$_5$]$_x$** crystal, data were obtained on a Bruker D8 GADDS/MWPC three-circle X-ray diffractometer (Cu Kα radiation, λ = 1.541 84 Å), also operating at 110 K. The structures were solved by direct methods. H atoms were added at idealized positions and refined with fixed isotropic displacement parameters equal to 1.2 times the isotropic displacement parameters of the atoms to which they were attached. Anisotropic displacement parameters were determined for all non-H atoms. The programs utilized were as follows: data collection and cell refinement for **Zn-1′-Ac**, *SHELXTL*;[26] data collection and cell refinement for **[Et$_4$N][(Zn-1′-Cl)W(CO)$_4$]**, *APEX-II*;[27] data collection and cell refinement for **[(Zn-1′-Ac)W(CO)$_5$]$_x$**, Bruker *FRAMBO*;[28] data reduction, *SAINT*;[29] absorption correction, *SADABS*;[30] structure solution and structure refinement for all structures, *SHELXS-97* and *SHELXL-97*;[26] molecular graphics and preparation of material for publication, *SHELXTL-PLUS*, version 6.14.[26] The final data presentation and structure plots were performed using *X-Seed*.[31] Table S1 (Supporting Information) lists the crystallographic data for the three compounds included in this report.

Scheme 1. Synthesis and Products

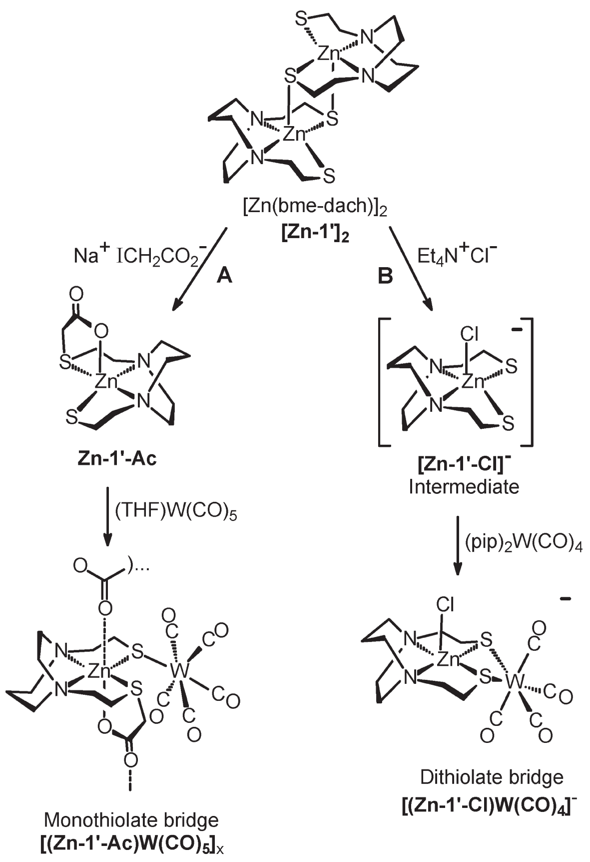

Results and Discussion

Scheme 1 displays the synthetic approach to monomeric zinc thiolates derived from the dimeric precursor **[Zn-1′]$_2$**.

---

[25] *SMART 1000 CCD*; Bruker Analytical X-ray Systems; Madison, WI, 1999.

[26] Sheldrick, G. *Acta Crystallogr.* **2008**, *A64*, 112–122 and references cited therein.

[27] *APEX II*, version 2008.6-0; Bruker-Nonius Inc.: Madison, WI, 2008.

[28] *FRAMBO*, version 4.1.13; Bruker-Nonius Inc.: Madison, WI, 2003.

[29] *SAINT*; Bruker-Nonius Inc.: Madison, WI, 2003.

[30] Sheldrick, G. *SADABS*; University of Göttingen: Göttingen, Germany, 2006.

[31] Barbour, L. J. *J. Supramol. Chem.* **2001**, *1*, 189–191.

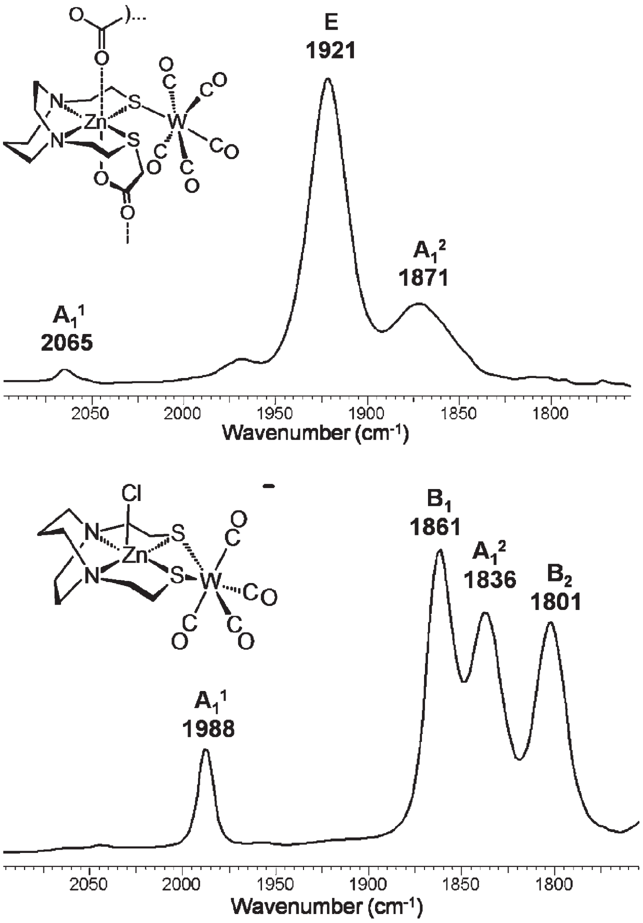

Figure 2. IR spectra of the ν(CO) region in a DMF solution. Top: **[(Zn-1′-Ac)W(CO)$_5$]$_x$**. Bottom: **[(Zn-1′-Cl)W(CO)$_4$]$^-$**.

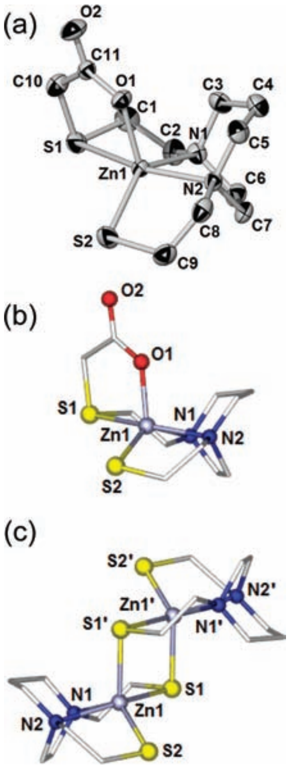

Figure 3. (a) Thermal ellipsoid plot of **Zn-1′-Ac** and (b) the ball-and-stick displays of **Zn-1′-Ac** and (c) the **[Zn-1′]$_2$** precursor. Selected metric parameters for comparison of **Zn-1′-Ac** and **[Zn-1′]$_2$** (in brackets). Bond lengths (Å): Zn1−S1, 2.587(3) [2.496(2)]; Zn1−S2, 2.263(2) [2.308(2)]; Zn1−N1, 2.159(3) (2.181(6)); Zn1−N2, 2.171(3) [2.274(5)]; Zn1−O1, 1.983(2); Zn1−S1′, 2.417(2). Bond angles (deg): N1−Zn1−N2, 75.21 (10) [71.94(19)]; S1−Zn1−S2, 107.72(4) [108.28(6)].

Because **[Zn-1′]$_2$** and the monomeric **Zn-1′-Ac** product are colorless, the cleavage reaction by path A was first monitored by thin-layer chromatography (TLC) on silica plates via iodine staining. Product separation was accomplished by silica column chromatography using MeOH as the eluent, and the retention factors from TLC plates were used to identify product-containing fractions. The solvent was removed from the consolidated product fractions, and the white powder, **Zn-1′-Ac**, was recrystallized for characterization and use in further reactions.

The photolytic conversion of $W(CO)_6$ to $(THF)W(CO)_5$ was monitored by FTIR spectroscopy following disappearance of the T_{1u} band of $W(CO)_6$ at 1974 cm^{-1} and growth of the 1930 cm^{-1} band of $(THF)W(CO)_5$. This golden solution was added to a **Zn-1′-Ac** suspension in THF. Following stirring for 3.5 h, all of the **Zn-1′-Ac** solid was pulled into the solution and the ν(CO) IR bands indicated conversion to a new species with absorptions as seen in Figure 2 (top). Yellow X-ray-quality crystals were obtained by layering a THF solution with hexane. This product was typically protected from air and moisture because it is more sensitive than the **Zn-1′-Ac** metalloligand. Nevertheless, the **[(Zn-1′-Ac)W(CO)$_5$]$_x$** product is stable to CO(g), as was demonstrated by exposure to bubbling CO(g) for extensive time periods at 22 °C in THF. Over the course of 6 days, approximately 30% conversion to $W(CO)_6$ was observed.

As shown in pathway B of Scheme 1, **[Et$_4$N]$^+$Cl$^-$** cleavage of the insoluble **[Zn-1′]$_2$** dimer resulted in the formation of **[Zn-1′-Cl]$^-$**, which was used in situ for the synthesis of **[(Zn-1′-Cl)W(CO)$_4$]$^-$**. The addition of the $(pip)_2W(CO)_4$ complex as a CH_2Cl_2 solution to **[Zn-1′-Cl]$^-$** resulted in a clear golden solution. The air-stable yellow solid obtained from this solution by hexane precipitation was washed with benzene and recrystallized by layering of a CH_2Cl_2 solution with hexane. The purified compound was redissolved in DMF to yield the IR spectra of the ν(CO) region given in Figure 2 (bottom).

Molecular Structures. Zn-1′-Ac. X-ray diffraction studies on the single crystals of **Zn-1′-Ac**, **[(Zn-1′-Ac)W(CO)$_5$]$_x$**, and **[(Zn-1′-Cl)W(CO)$_4$]$^-$** yielded the molecular structures shown in Figures 3−7, with selected metric parameters listed in Table 2. Figure 3 displays the **Zn-1′-Ac** monomeric complex as a thermal ellipsoid plot (a) and a ball-and-stick graphic (b), and the **[Zn-1′]$_2$** precursor (c)[18] is also shown for comparison. Views b and c highlight the diazacycle scaffolds and the flexibility of the pendant mercaptoethylene arms, which in combination with the metal's geometry preference accounts for the distorted square-pyramidal structure. The three carbon N-to-N linker of the diazacycloheptane ring in **Zn-1′-Ac** lies on the same side of the N_2S_2 donor set as the acetate arm does. Note that the pendant arms in both the **Zn-1′-Ac** and the **[Zn-1′]$_2$** structures are staggered across the N_2S_2 planes. Both compounds contain five-coordinate Zn centers with similar ∠N1−Zn1−N2 (72−75°) and ∠S1−Zn1−S2 (108°) within the bme-dach portion of the ligand. For both, the Zn−S2$_{\text{terminal}}$ distance is shorter than the remaining Zn−S1 distance (the μ-S in **[Zn-1′]$_2$** and the thioether S in **Zn-1′-Ac**). The N_2S_2 donor set

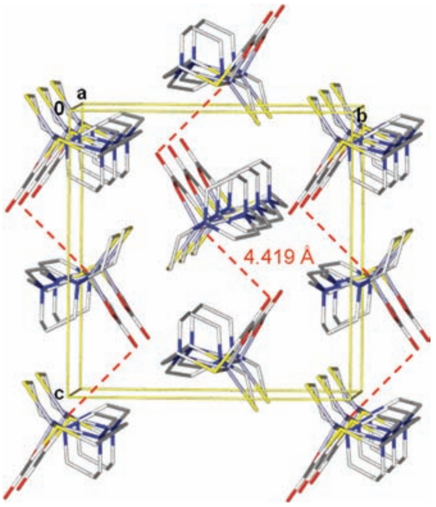

Figure 4. **Zn-1′-Ac** unit cell displaying the closest intermolecular Zn−O distances in the *bc* plane. All other Zn—O intermolecular distances are >6 Å.

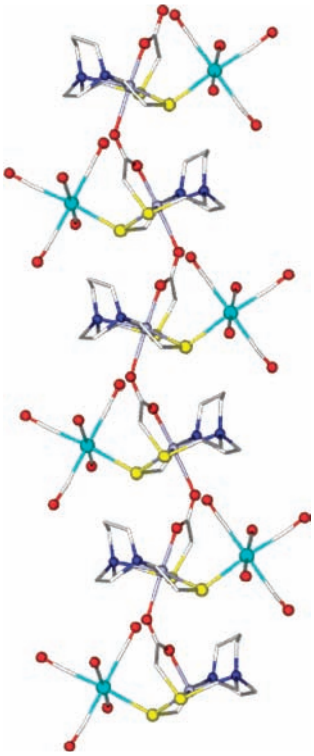

Figure 5. Ball-and-stick representation of the molecular structure of **[(Zn-1′-Ac)W(CO)$_5$]$_x$**, a coordination polymer.

within the **Zn-1′-Ac** complex (without Zn) forms an irregular "plane" with an average atom deviation of 0.306 Å. Analysis of the bond angles according to ideal square-pyramidal (τ = 0) versus ideal trigonal-bipyramidal (τ = 1) geometries yields a τ value of 0.36 for **Zn-1′-Ac**. According to Addison et al., this value more closely approaches the square-pyramidal geometry, while that for the **[Zn-1′]$_2$** structure (τ = 0.47) is an almost exact intermediate between the square-pyramidal and trigonal-bipyramidal geometries.[18,32]

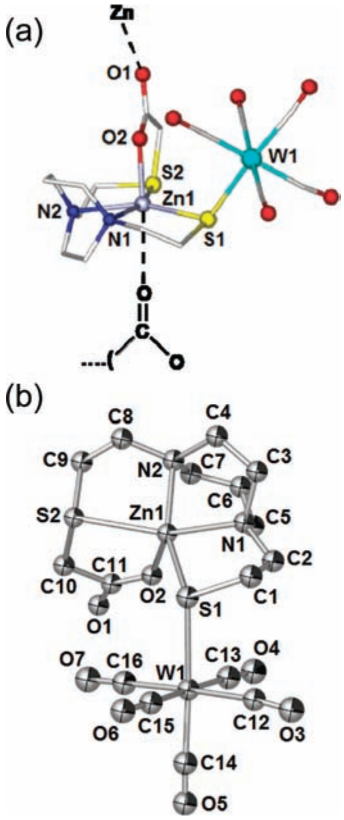

Figure 6. Two views of the repeat unit in the Zn(μ-SR)W coordination polymer: (a) a ball-and-stick representation, where the dashed line represents the intermolecular Zn—O contact to an adjacent unit, and (b) a thermal ellipsoid plot of the **[(Zn-1′-Ac)W(CO)$_5$]** unit within the coordination polymer.

Because the sizable collection of previously reported NiN_2S_2 complexes have demonstrated an ideal use of the N_2S_2 diazacycle ligand systems for nearly perfect square-planar geometry,[33,34] the structures reported here add to the examples in which these systems demonstrate flexibility and positive response to the geometrical preferences of the central metal ion. Nevertheless, the hydrocarbon backbone portion of the N_2S_2 ligands has important effects on the overall geometry as well. For example, the five-coordinate **Zn-1′-Ac** geometry is analogous to that of the product of the cleavage reaction of [Zn(bme-daco)]$_2$, **[Zn-1]$_2$**, with $ClCH_2CO_2H$.[35] The resulting five-coordinate **Zn-1-Ac** complex has a τ value of 0.12, i.e., substantially square pyramidal in geometry. It should be noted that the packing diagram of the **Zn-1-Ac** analogue contains H_2O molecules hydrogen bonded to the carboxylate O atoms within its crystallographic unit cell.

The crystal packing of **Zn-1′-Ac** molecules (Figure 4) finds no Zn−O or Zn−S intermolecular distances less than 4.419 Å. Thus, the packing diagram shows no intermolecular interactions that might indicate acetate bridging to neighboring Zn centers. In contrast, interactions between

---

[32] Addison, A. W.; Rao, T. N.; Reedijk, J.; van Rijn, J.; Verschoor, G. C. *J. Chem. Soc., Dalton Trans.* **1984**, *7*, 1349–1356.

[33] Smee, J. J.; Miller, M. L.; Grapperhaus, C. A.; Reibenspies, J. H.; Darensbourg, M. Y. *Inorg. Chem.* **2001**, *40*, 3601–3605.

[34] Rampersad, M. V.; Jeffery, S. P.; Golden, M. L.; Lee, J.; Reibenspies, J. H.; Darensbourg, D. J.; Darensbourg, M. Y. *J. Am. Chem. Soc.* **2005**, *127*, 17323–17334.

[35] Goodman, D. C.; Tuntulani, T.; Farmer, P. J.; Reibenspies, J. H.; Darensbourg, M. Y. *Angew. Chem., Int. Ed. Engl.* **1993**, *32*, 116–119.

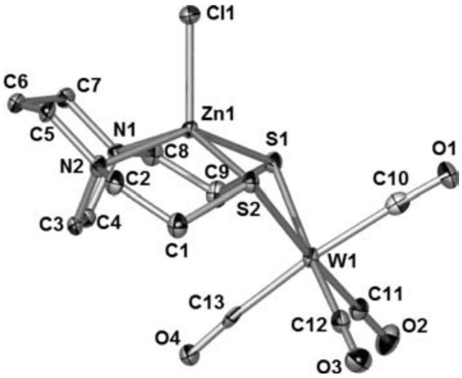

Figure 7. Thermal ellipsoid plot of **[(Zn-1′-Cl)W(CO)$_4$]$^-$**. The Et_4N^+, H_2O and CH_2Cl_2 molecules within the crystal lattice have been removed from this illustration for clarity. In addition to metric parameters displayed in Table 2: Bond length (Å): Zn(1)−Cl(1), 2.2902(12). Bond angle (deg): S(1)−W(1)−S(2), 82.34(3).

Table 2. Selected Bond Lengths [Å] and Angles [deg] for **Zn-1′-Ac**, **[(Zn-1′-Ac)W(CO)$_5$]$_x$**, and **[(Zn-1′-Cl)W(CO)$_4$]$^-$**

	Zn-1′-Ac	**[(Zn-1′-Ac)W(CO)$_5$]$_x$**	**[(Zn-1′-Cl)W(CO)$_4$]$^-$**
Zn−N^c	2.165(3)	2.199(2)	2.207(4)
Zn−S$_{thiolate}$	2.263(2)		
Zn−S$_{thioether}$	2.587(3)	2.548(7)	
Zn−S$_W$		2.403(7)	2.395(12)^c
Zn−O	1.983(2)	2.074(2)^a 2.265(2)^b	
W−S		2.591(7)	2.591(2)^c
∠S−Zn−S	107.72(4)	112.6(3)	90.84(4)
∠N−Zn−N	75.21(10)	74.1(7)	73.21(13)
∠Zn−S−W		120.0(3)	125.9^d

^{a} Intramolecular. ^{b} Intermolecular. ^{c} Average distance. ^{d} Hinge angle, defined in the text.

Zn-1′-Ac units are extensive in the **[(Zn-1′-Ac)W(CO)$_5$]$_x$** complex described next.

[(Zn-1′-Ac)W(CO)$_5$]$_x$. As illustrated in Figure 5, the structure of **[(Zn-1′-Ac)W(CO)$_5$]$_x$** is that of a coordination polymer involving the **Zn-1′-Ac** unit, in which the acetate group serves as a bridging ligand between Zn atoms in adjacent molecules, utilizing both O atoms and resulting in six-coordinate Zn centers. The repeating units propagate along the *b* axis of the crystal lattice. The intra- and intermolecular Zn−O distances are 2.074(18) and 2.265(17) Å, respectively.

Figure 6 presents two views that emphasize the orientation of $W(CO)_5$ with respect to the **Zn-1′-Ac** metalloligand of the coordination polymer repeat unit. Notably, $W(CO)_5$ resides on the same side as the acetate arm, which emanates from S2 as the μ-S bridge is created from S1. In terms of the extended structure of the coordination polymer, this results in an alternation of $W(CO)_5$ units along the zinc acetate chain. The ∠Zn1−S1−W1 angle of 120.0(3)° places the $W(CO)_5$ moiety beyond steric interactions, which is consistent with the regular C_{4v} $LW(CO)_5$ geometry suggested by the ν(CO) IR spectrum (Figure 2). The $W(CO)_5$ moiety is bound by the single S1 thiolate of **Zn-1′-Ac** at a S1−W1 distance of 2.591(7) Å. The Zn−S$_{thiolate}$ distance of 2.403(7) Å is approximately 0.15 Å longer than that in the free **Zn-1′-Ac** compound. As expected, the Zn−S$_{thioether}$ distance of 2.548(7) Å in **[(Zn-1′-Ac)W(CO)$_5$]$_x$** is largely the same as that in the free **Zn-1′-Ac**, 2.587(3) Å. The Zn1−O2 distance for the **Zn-1′-Ac** unit within the coordination polymer is approximately 0.1 Å longer than the Zn−O$_{intramolecular}$ distance in the free **Zn-1′-Ac**.

[(Zn-1′-Cl)W(CO)$_4$]$^-$. The Et_4N^+ salt of **[(Zn-1′-Cl)W(CO)$_4$]$^-$** was prepared according to the procedure outlined as route B in Scheme 1 and isolated from a CH_2Cl_2 solution layered with hexane. The structure of the anion is given in Figure 7. It consists of a square-pyramidal $ZnN_2S_2Cl^-$ unit serving as a bidentate ligand to $W(CO)_4$. In contrast to the five-coordinate **Zn-1′-Ac** structures, the $ZnN_2S_2Cl^-$ portion of the adduct finds the N_2S_2 donor set as a nearly ideal square plane with a mean deviation of 0.0046 Å. The Zn atom is displaced from the N_2S_2 plane by 0.7436 Å toward the apical chloride with a Zn1−Cl1 distance of 2.2902(12) Å. The angulation of a metal dithiolate to an exogenous ion or species interaction is expressed as a “hinge” angle. In this case, it is defined as the angle between the N1−N2−S1−S2 (without Zn) best plane and the S1−S2−C11−C12 (without W) plane, 125.9°. If defined by the Zn1−S1−S2 and W1−S1−S2 plane intersections, the angle is 150.4°.

Both thiolate S atoms are bound to $W(CO)_4$ at S1−W1 and S2−W1 distances of 2.5915(11) and 2.5912(11) Å. The S−W distance within **[(Zn-1′-Cl)W(CO)$_4$]$^-$** is identical with that found within **[(Zn-1′-Ac)W(CO)$_5$]$_x$** described above. Furthermore, Zn1−S1 and Zn1−S2 distances of 2.3845(11) and 2.4055(12) Å are not significantly different from the Zn−S$_{thiolate}$ distance [2.403(7) Å] in **[(Zn-1′-Ac)W(CO)$_5$]$_x$**.

The **[(Zn-1′-Cl)W(CO)$_4$]** dithiolate-bridged complex contains several structural features comparable to those of the [(Zn(bme-dach)Cl)(Pt(dien))]$^+$ adduct, shown in parts d and b of Figure 1, respectively. The Zn displacement of 0.7436 Å from the N_2S_2 best plane within **[(Zn-1′-Cl)W(CO)$_4$]$^-$** is similar to that found in the **[Zn-1′-Cl]$^-$** unit of [(Zn(bme-dach)Cl)(Pt(dien))]$^+$, 0.8628 Å.[18] The dithiolate-bridged Zn−S bond distances in **[(Zn-1′-Cl)W(CO)$_4$]$^-$** are slightly shorter than those found within the Pt^{II} adduct [2.4567(10) and 2.4210(10) Å]. A comparison of the hinge angles, defined above (without Zn or Pt centers), finds a more acute angle of 107.2° for the Pt derivative. The hinge angles have also been established in a series of $(NiN_2S_2)W(CO)_4$ complexes to range between 107 and 136°, depending largely on the intramolecular steric interactions.[34,36] Comparisons to selected Ni derivatives are also presented in the IR spectroscopy discussion below.

IR Spectroscopy. Because the Zn−Pt thiolate-bridged derivatives have provided structural investigations of heavy-metal adducts,[18] the CO ligand incorporation into the Zn−W adducts permits spectral identification of the complexes via IR spectroscopy. The $LW(CO)_5$ complexes have three ν(CO) IR-active bands, as seen at the bottom of Figure 2, shifted to higher wavenumbers from those observed from the $L_2W(CO)_4$ analogues. Interestingly, there is little difference in ν(CO) values between the anionic **[Zn-1′-Cl]$^-$** as a monodentate donor and the neutral **Zn-1′-Ac** S-donor metalloligand (Table 3). We conclude that in the latter the modification of the thiolate to a thioether is compensated for by the addition of the

---

(36) Phelps, A. L.; Rampersad, M. V.; Fitch, S. B.; Darensbourg, M. Y.; Darensbourg, D. J. *Inorg. Chem.* **2006**, *45*, 119–126.

Table 3. CO Stretching Frequencies (cm^{-1}) and Assignments for W(CO)$_4$ (pseudo-C_{2v}) and W(CO)$_5$ (pseudo-C_{4v}) Derivatives of Zinc(II) and Nickel(II) Thiolate Metalloligands

$L^{\frown}LW(CO)_4$	solvent	$A_1{}^1$	B_1	$A_1{}^2$	B_2
[Zn-1′Cl]$^-$	DMF	1988	1861	1836	1801
[Zn-1′Cl]$^-$	CH_2Cl_2	1990	1863	1845	1800
[Ni-1′][a]	DMF	1996	1873	1852	1817
[Ni-1*][b]	DMF	1996	1871	1857	1816
[Ni-ema]$^{2-}$[c]	DMF	1986	1853	1837	1791

$LW(CO)_5$	solvent	$A_1{}^1$	E	$A_1{}^2$
THF	THF	2075	1930	1891
Zn-1′-Ac	THF	2065	1925	1888
Zn-1′-Ac	DMF	2065	1921	1871
Zn-1′-Ac	solid	2059	1910	1867 (sh 1807)
[Zn-1′Cl]$^-$	DMF	2063	1920	1869
[Zn-1′Cl]$^-$	CH_2Cl_2	2064	1921	1863
[Ni-1*]	DMF	2061	1920	1874

[a] **[Ni-1′]** = [*N*,*N*′-bis(2-mercaptoethyl)-*N*,*N*′-diazacycloheptane]nickel(II). [b] **[Ni-1*]** = [*N*,*N*′-bis(2-mercapto-2-methylpropane-*N*,*N*′-diazacyclooctane]nickel(II). [c] **[Ni-ema]$^{2-}$** = [*N*,*N*′-ethylenebis(2-mercaptoacetamide)]nickel(II).[34,36,39]

O donor to Zn, rendering the available thiolate S donor nearly as electron-rich as that in the anionic chlorozinc ligand.

The ν(CO) IR spectra of the tungsten carbonyl derivatives, M(μ-SR)$_2$W(CO)$_4$ and M(μ-SR)W(CO)$_5$, display the requisite number of bands as predicted for idealized C_{2v} and C_{4v} symmetry, respectively.[37] Despite the severe asymmetry of the monodentate **[Zn-1′-Cl]$^-$** and **Zn-1′-Ac** ligands, the ν(CO) IR spectra are not distorted from those of typical LW(CO)$_5$ in which L is a symmetrical ligand. This is not uncommon but, nevertheless, noteworthy.

As listed in Table 3, the observed ν(CO) frequencies for **[(Zn-1′-Ac)W(CO)$_5$]$_x$** remained relatively consistent in various solvents and the ν(CO) solid-state values showed more complexities as expected but are, nevertheless, quite similar. Because the W(CO)$_5$ unit does not report on the degree of aggregation in solution versus solid state, the carboxylate region was examined for possible insight into the intramolecular interactions between **[(Zn-1′-Ac)W(CO)$_5$]** units. The IR spectra of the acetate region in free **Zn-1′-Ac** and in **[(Zn-1′-Ac)W(CO)$_5$]$_x$** illustrated multiple bands in the 1400 cm^{-1} range, which have not been assigned, and a high-frequency band in the 1590–1650 cm^{-1} range, indicative of unidentate carboxylate coordination, as observed in classical metal acetate complexes.[38] The higher frequency band of **[(Zn-1′-Ac)W(CO)$_5$]$_x$** at 1592 cm^{-1} in the solid-state spectrum shifts to 1653 cm^{-1} when dissolved in THF, a value consistent with the free **Zn-1′-Ac** (1636 cm^{-1} in CH$_3$CN), and suggests dissociation into discrete **[(Zn-1′-Ac)W(CO)$_5$]** units in solution.

A wide range of Ni(N$_2$S$_2$) complexes have been well-studied as metalloligands to tungsten carbonyl complexes and their ν(CO) frequencies used to indicate their electron-donating abilities.[34,36,39] Data points from these studies are included for comparison to the **[Zn-1′-Cl]$^-$** and **Zn-1′-Ac** metalloligands in Table 3. The four ν(CO) values for the anionic **[(Zn-1′-Cl)W(CO)$_4$]$^-$** are positioned 8–16 cm^{-1} lower than those of the neutral **[(Ni-1′)(μ-SR)$_2$W(CO)$_4$]** analogue. This result is consistent with the overall charge on the heterobimetallic; notably, the dianionic [(Ni-ema)W(CO)$_4$]$^{2-}$ [ema = *N*,*N*′-ethylenebis(2-mercaptoacetamide)] has ν(CO) IR bands some 10 cm^{-1} lower.

Zn–W Di- to Monothiolate-Bridged Adducts: CO(g) Addition. In addition to the IR spectral comparisons to the nickel(II) thiolate analogues above, the **[(Zn-1′-Cl)W(CO)$_4$]$^-$** complex was probed for its Zn(μ-SR)$_2$W bridge stability under CO(g) purging, as was carried out for **[Ni-1*]W(CO)$_4$**.[34,36] The dithiolate-bridged **[Ni-1*]W(CO)$_4$** [[*N*,*N*′-bis(2-mercapto-2-methylpropane-*N*,*N*′-diazacyclooctane]nickel(II)] complex listed at the top of Table 3 was placed under a CO(g) atmosphere to monitor its conversion to the monothiolate adduct (listed at the bottom of Table 3). The Ni complex in a DMF solution was pressurized with 400–1400 psi of CO(g) (at various temperatures) in a stainless steel Parr reactor and the ν(CO) region monitored by IR spectroscopy. These studies concluded that the **[Ni-1*]W(CO)$_4$** dithiolate adduct was readily converted to the **[Ni-1*]W(CO)$_5$** monothiolate bridge via a ring-opening process. However, the **[Ni-1*]W(CO)$_5$** species was extremely stable toward further W–S bond cleavage and CO ligand substitution.

Scheme 2 displays the reaction of the **[(Zn-1′-Cl)W(CO)$_4$]$^-$** complex with CO(g), 1 atm in DMF solution at 22 °C. Consistent with CO(g) addition to the Ni^{II} complex, the dithiolate-bridged **[(Zn-1′-Cl)W(CO)$_4$]$^-$** readily formed the monothiolate adduct under these conditions. Furthermore, the addition of CO(g) for over a period of 6 days showed minimal formation of W(CO)$_6$ (at 1972 cm^{-1}), suggesting the great stability of the monothiolate metalloligand toward loss and CO exchange. IR spectral overlays of the ν(CO) frequencies during CO(g) bubbling in DMF and CH$_2$Cl$_2$ solutions are provided in the Supporting Information.

Comments and Conclusions

The bme-dach ligand, known for its square-planar N$_2$S$_2$ donor set in d^8 transition-metal complexes, displays

---

[37] Cotton, F. A.; Kraihanzel, C. S. *J. Am. Chem. Soc.* **1962**, *84* 4432–4438.

[38] Cotton, F. A.; Wilkinson, G. *Advanced Inorganic Chemistry: A Comprehensive Text*, 3rd ed.; Interscience: New York, 1972; pp 620–681.

[39] Rampersad, M. V.; Jeffery, S. P.; Reibenspies, J. H.; Ortiz, C. G.; Darensbourg, D. J.; Darensbourg, M. Y. *Angew. Chem., Int. Ed.* **2005**, *44*, 1217–1220.

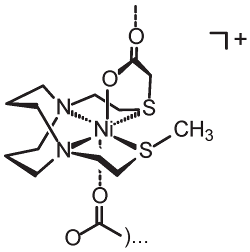

Figure 8. NiN$_2$S$_2$′OO′ subunit within the Ni^{2+} coordination polymer, [*N*-(3-thiabutyl)-*N*′-(3-thiapentanoate)-1,5-diazacyclooctane]nickel(II) iodide.[40]

Scheme 2

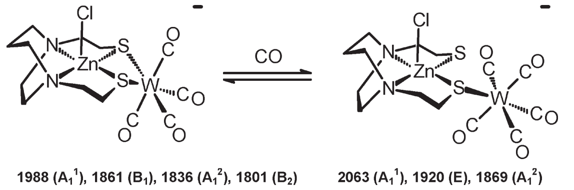

considerable flexibility according to the geometrical preferences of Zn^{II} in the compounds characterized herein. A square pyramid is observed in the **[(Zn-1′-Cl)W(CO)$_4$]$^-$** complex where Zn is significantly displaced from the N$_2$S$_2$ plane and toward the apical chloride. In contrast, the **[Zn-1′]$_2$** and **Zn-1′-Ac** complexes are five-coordinate and exhibit seriously distorted geometries, with the latter significantly rearranging in the W(CO)$_5$ adduct. **[(Zn-1′-Ac)W(CO)$_5$]$_x$** utilizes an additional O-atom interaction at the Zn atom, which generates an octahedral ZnN$_2$SS′O$_2$ structure, defining a coordination polymer, with the W(CO)$_5$ units decorating the **[Zn-1′Ac]$_n$** chain. The role of W(CO)$_5$ in inducing the bridging carboxylate interaction that defines the coordination polymer would appear to be electronic. The W−S interaction reduces the electron-donor character of the thiolate, enhancing the electrophilicity of the Zn atom within **Zn-1′-Ac**, and thus results in the attraction of an adjacent carboxylate.

Such a coordination polymer is not without precedent. In fact, S modification of a similar N$_2$S$_2$ complex of Ni^{II}, Ni (bme-daco), by methylation of one thiolate S allowed for the remaining S to react with a single iodoacetate, producing a paramagnetic NiN$_2$S$_2$′OO′ coordination polymer (Figure 8).[40] Reminiscent of the zinc polymer, the nickel compound contains an O atom of a neighboring cation that occupies the sixth coordination site on the central Ni^{II}. This result again demonstrates that S modification may have a major effect on the structural diversity. Because the nickel complex forms a coordination polymer after S-methylation, the zinc analogue does so as a result of S-bridging to tungsten. This also points to the connection between S-alkylation and S-metalation, as noted in the Introduction, for the interactions of Zn-bound thiolates with methyl (Ada protein) and platinum (chemotherapeutic) species.

Grapperhaus et al. have reported two studies in which nickel and zinc are compared in precisely the same N$_2$S$_2$ ligand donor set.[12,13] The studies of S-oxygenation and S-alkylation concluded that the effects of electrostatic interactions prevalent in the Zn^{2+} derivative and the π-antibonding interactions in the Ni^{2+} complexes served in the former to protect the thiolate while the latter activated the thiolate. Our studies of alkylation and metalation suggest that nickel and zinc thiolates have similar reactivity, electronic effects as metalloligand donors, and templating effects toward ligand modification.

The distorted N$_2$S$_2$ “plane” (average atom deviation of 0.306 Å) within **Zn-1′-Ac** holds the central Zn displaced by 0.447 Å from the irregular plane. With formation of the coordination polymer, the N$_2$S$_2$ best plane transforms to an average atom deviation of only 0.131 Å, and the Zn is displaced by only 0.146 Å. Such metric shifts resulting from five- to six-coordinate geometries may occur in macromolecules, and possibly in proteins, in which long-range structural consequences could be considerable. Because the coordination environments about Zn in many Zn-bearing biomolecules are uncertain, we merely note the possible interactions, geometries, and coordination spheres that the small ion is amenable to accommodate and shift between.

Zinc is shown to template the bme-dach ligand into a *cis*-di- and monothiolato S-donor ligand to heavy-metal tungsten carbonyl derivatives. There is considerable significance to this finding because metal carbonyls are well-known as biomarkers through the sensitivity of their IR-active, isolated CO stretching vibrations.[41,42] The stability of the Zn (μ-SR)W(CO)$_x$ bond suggests promise for application of such biomarkers toward the notoriously silent zinc in *S*-cysteinyl environments.

Acknowledgment. The authors gratefully acknowledge the financial support of the National Science Foundation (Grant CHE-0616695) and the R. A. Welch Foundation (Grant A-0924). We thank Ross Nearburg for the synthesis of a portion of the **Zn-1′-Ac** supply needed for the tungsten carbonyl reactions.

Supporting Information Available: Table of crystallographic data collection and refinement, packing diagrams of the crystal structures, IR spectra of CO(g) addition in DMF and CH$_2$Cl$_2$ solutions, and X-ray crystallographic data in CIF format. This material is available free of charge via the Internet at http://pubs.acs.org. CCDC 718636, 718637, and 718638 contain the supplementary crystallographic data for this paper. These data can be obtained free of charge via www.ccdc.cam.ac.uk/data_request/cif or by emailing data_request@ccdc.cam.ac.uk or contacting The Cambridge Crystallographic Data Centre, 12, Union Road, Cambridge CB2 1EZ, U.K.; fax +44 1223 336033.

---

(40) Goodman, D. C.; Farmer, P. J.; Reibenspies, J. H.; Darensbourg, M. Y. *Inorg. Chem.* **1996**, *35*, 4989–4994.

(41) Metzler-Nolte, N. *Angew. Chem., Int. Ed.* **2001**, *40*, 1040–1043.

(42) *Bioorganometallics: Biomolecules, Labeling, Medicine*; Jaouen, G., Ed.; Wiley-VCH Verlag GmbH & Co. KGaA: Weinheim, Germany, 2006; pp 202−205 and 220−226.